



Mixed Convection in a Casson Fluid Flow towards a Heated Shrinking Surface

Haider Ali¹, Ghulam Shabir², Zubair Ahmad², Yasir Qayyum¹ and Ather Qayyum^{1,*}

¹Department of Mathematics, Institute of Southern Punjab, Multan, Pakistan

e-mail: atherqayyum@isp.edu.pk*

²Department of Mathematics, University of Agriculture, Faisalabad, Pakistan

Abstract

In this paper, an extensive analysis of mixed convection effects on steady two-dimensional stagnation point flow of a Casson fluid over a heated horizontal sheet has been numerically investigated. The governing Navier-Stokes equations of the present problem are transformed into nonlinear ordinary differential equations by applying a similarity transformation. A numerical solution of the problem has been obtained by employing the linearization technique along with the finite difference discretization. The impact of the Casson fluid parameter, the thermo-radiative parameter, the mixed convection parameter, the slip parameter, and the Prandtl number on the fluid motion and temperature is studied through graphical data. The convection parameter, the slip parameter and the Casson fluid parameter tends to accelerate the flow. The temperature distribution is however reduced by the convection parameter, slip parameter, thermal radiation and the Prandtl number.

This work is based on [25] in which micropolar fluid flow over a heated surface was investigated by using the homotopy analysis method. We have extended the problem by considering the combined impact of mixed convection and thermal radiation on the Casson fluid flow towards a heated shrinking sheet, by using a numerical method.

Introduction

Fluids can be categorized as per the viscosity concept in two groups of Newtonian fluidics and non-Newtonian fluidics. Research into this area has been developed by the extensive uses of non-Newtonian fluids in different disciplines of engineering and

Received: July 4, 2023; Revised & Accepted: July 31, 2023; Published: August 9, 2023

2020 Mathematics Subject Classification: 76B75, 76D55, 76N25.

Keywords and phrases: stagnation flow, heat transfer, Casson fluid, shrinking sheet.

*Corresponding author

Copyright © 2023 the Authors

industry. The flow patterns of Casson fluidic are investigated in this paper with different flow assumptions.

The physics of non-Newtonian fluid flows is widely considered to be a unique challenge to scientists, mathematicians, and engineers. Because of the complexity of these fluids, there is no one constitutive equation that illustrates all of their properties. Many non-Newtonian fluid models have been developed over the process. Among these, the Casson fluid [1] has piqued the public's curiosity. The yield stress is present in the Casson fluid. Casson fluid is widely known to be a shear-thinning fluid [2,3], and it acts like a solid while the yield stress is greater than the shear stress, but it begins to move when the shear stress is high [4].

Obalalu et al. [5] analytically and quantitatively showed the compressed Casson fluid flow with heat radiation. A differential system was used to regulate the model, which proved successful. As a consequence of the analysis, the following observations were made. They observed that the presence of squeeze numbers is critical, and that raising the squeezing parameter enhances the temperature of the fluid. Higher values of variable viscosity have a substantial effect on skin friction.

Reddy et al. [6] have examined the growth of heat transfer rate in Casson fluidic over the upper surface of a parabolic volume. Oyelakin et al. [7] considered the unstable two-dimensional viscous flow of Casson nanofluid via a stretched surface with the control of buoyant force and radiation of heat. Ullah et al. [8] examined the heat transfer rate of Casson with suspended nano-sized particles through wedge-shaped objects with effects of various body forces like buoyancy and Lorentz force.

There are a lot of reviews existing in the literature of non-Newtonian fluids for the flow and thermal transfer analysis with varying boundary conditions and thermos physical parameters, (see [9-17]).

Casson fluid could be described as a shear diminishing fluid, assuming that it has a non-flowing infinite viscosity, under low values of yield stress, there is no flow and an infinite shear rate with no viscosity. Casson fluid is also regarded as an infinite-viscosity dilatant fluid at null shear values. The pattern of Casson fluid is used for characterizing the behavior of the non-Newtonian fluidic. In the temperature field equation, thermal radiation expression will be used. Numerical results of these equations are then achieved. In particular, stretching/shrinking surfaces with different non-Newtonian fluids have many practical uses in metallurgical instrumentations, polymer dispensation, food

production, boiler, biotech, biomedical devices, artificial heat designing, etc. [18-19]. Magyari and Keller [20] considered the boundary stream-line flow of non-Newtonian fluid over a nonlinearly stretching surface with a variable temperature distribution and obtained analytical and numerical solutions simultaneously.

Pramanik [21] used a porous stretching sheet to examine the thermal effects on flow and heat transfer in Casson fluid in the presence of suction/injection at the surface. Bhattacharya et al. [22] scrutinized the slip boundary flow effects on the Casson fluidic over an impervious shrinking sheet.

Our efforts in this work are to discuss the behaviour of a novel prototype for the Casson fluid to analyze the mixed convection flow in the vicinity of stagnation point through a heated shrinking surface. The impact of buoyant forces on the boundary stream-line flow with velocity slip parameter would be examined numerically by applying the quasi-linearization method embedded with a finite difference algorithm based on MATLAB simulation tools used in the works of Ali et al. [23,24].

This research paper presents a novel numerical investigation of mixed convection effects on the two-dimensional stagnation point flow of a Casson fluid over a heated horizontal sheet. By considering the combined impact of mixed convection and thermal radiation, the study extends the findings of a previous work on micropolar fluid flow. The analysis employs a similarity transformation and linearization technique for solving the governing Navier-Stokes equations, providing valuable insights into the influence of various parameters on fluid motion and temperature distribution. This study contributes to the understanding of complex fluid dynamics and heat transfer phenomena, presenting significant implications for engineering applications involving Casson fluids and similar systems.

Mathematical Modeling and Numerical Solution

Let start with the governing equations of the problem:

$$\frac{\partial v_1}{\partial x} + \frac{\partial v_2}{\partial y} = 0 \quad (1)$$

$$v_1 \frac{\partial v_1}{\partial x} + v_2 \frac{\partial v_1}{\partial y} = -\frac{1}{\rho} \frac{\partial p}{\partial x} + \nu \left(1 + \frac{1}{\beta} \right) \frac{\partial^2 u}{\partial y^2} + g\beta(T - T_\infty) \quad (2)$$

$$\rho C_p \left(v_1 \frac{\partial T}{\partial x} + v_2 \frac{\partial T}{\partial y} \right) = k_0 \frac{\partial^2 T}{\partial y^2} - \frac{\partial q_r}{\partial y}. \quad (3)$$

The boundary conditions for the velocity and temperature analysis of the Casson fluid

are:

$$\left. \begin{aligned} v_1(x, 0) &= u_w + u_s, \quad v_2(x, 0) = 0, \quad T(x, 0) = T_0 \\ v_1(x, \infty) &= U = ax, \quad T(x, \infty) = T_\infty \end{aligned} \right\} \quad (4)$$

We use the following new variables to transform the proposed model:

$$\left. \begin{aligned} \zeta &= \sqrt{\frac{a}{v}} y, \quad P(x, \infty) = P_0 - \frac{\rho a^2}{2} (x^2 + y^2), \quad \theta(\zeta) = \frac{T - T_\infty}{T_0 - T_\infty} \\ v_1(x, y) &= ax f'(\zeta), \quad v_2(x, y) = -\sqrt{av} f(\zeta) \end{aligned} \right\} \quad (5)$$

Eq. (1) is uniformly satisfied under the similarity transformation defined in eq. (5) and justifying the possible fluid motion.

The radiative function of heat flux q_r is formulated by conferring to the Rossland approximation equation defined as

$$q_r = \frac{-4\sigma^\circ}{3k_1^\circ} \frac{\partial T^4}{\partial y}, \quad (6)$$

where σ° is the Stefan-Boltzman constant and k_1° is the absorption coefficient. T^4 can be expressed as a linear function of temperature. Taylor series can be employed to expand T^4 about T_∞ and truncating the order greater than T^4 -terms, we have

$$T^4 = 4T_\infty^3 T - 3T_\infty^4. \quad (7)$$

Applying eq. (5) in eq. (2) and eq. (3), we found the following set of ODEs:

$$\left(1 + \frac{1}{\beta}\right) f'''' + f f'' - f'^2 + \lambda\theta + 1 = 0, \quad (8)$$

$$\left(R + \frac{4}{3}\right) \theta'' + R P_r f \theta' = 0. \quad (9)$$

Conditions on the boundaries in eq. (4) in view of the transformation set given in eq. (5) can be written as:

$$f(0) = 0, \quad f'(0) = \frac{b}{a} = \alpha + SLf'', \quad f'(\infty) = 1, \quad \theta(0) = 1, \quad \theta(\infty) = 0. \quad (10)$$

Here

$Pr = \frac{\mu c_p}{\kappa_0}$ is the Prandtl number, $R = \frac{k_0 k_1^\circ}{4\sigma T_\infty^3}$ is the thermal radiative parameter, $\lambda = \frac{Gr_x}{(Re_x)^2}$ is the buoyancy parameter (where $Gr_x = \frac{g\beta_0(T_0 - T_\infty)x^3}{\nu^2}$ is the Grashoff number and $Re_x = \frac{Ux}{\nu}$ is the Reynold number).

Methodology

For solving the transformed set of ODEs (with one being non-linear in nature), we consider two sequences of vectors $\{f^{(p)}\}$ and $\{\theta^{(p)}\}$ which converge to the numerical solutions of the above equations. The first one is obtained by linearizing eq. (7) as follows:

$$\begin{aligned} & \left(1 + \frac{1}{\beta}\right) f^{(p+1)''''} + f^{(p+1)''} f^{(p)} - 2f^{(p+1)'} f^{(p)'} + f^{(p+1)'} f^{(j)''} \\ & = (f^{(p)'})^2 - f^{(p)} f^{(p)''} + \lambda \theta^{(p+1)} + 1. \end{aligned} \quad (11)$$

Eq. (11) brings about a linear system of ordinary differential equations with f^p as a numerical solution of p^{th} equation. Linear ODEs obtained can be solved numerically by discretization using the central differences.

On the other hand, the heat equation is linear and the sequence $\{\theta^{(p)}\}$ can be generated as:

$$\left(1 + \frac{4}{3}R\right) \theta^{(p+1)''} + RPr f^{(p+1)} \theta^{(p+1)'} = 0. \quad (12)$$

This algebraic system of equations resulting after discretization may be solved by many well-known numerical techniques (for example, the successive over relaxation method or Gauss elimination method with Pivoting, to ensure stability).

Results and Discussion

In this section of the paper, we provide a visual display of our numerical findings to analyse the impact of the governing parameters on the thermal and flow characteristics of the problem. For a better understanding of the thermo-physical properties of the flow, we have focused on the impacts of the Casson fluid parameter β , the thermal radiation parameter R , the mixed convection parameter λ , the slip parameter SL , the shrinking/stretching parameter α , and the Prandtl number Pr .

Influence of the Casson fluid parameter β on the normal velocity and stream-wise velocity profiles is illustrated in Figures 1-2. From the graphs, it is clear that both velocity components tend to increase by enhancing the values of the Casson fluid parameter β . Further, it may be noted from the governing equations that, as $\beta \rightarrow \infty$, the nature of fluid tends to the pure Newtonian fluid.

Figures 3-5 represent the effect of the mixed convection parameter λ on both the components of velocity and the temperature profile as well. It has been perceived from the graphs, the growth in the value of λ causes a remarkable raise in the velocity profiles. It is obvious fact that the buoyant forces accelerate the fluid motion. The influence of λ on the temperature distribution is relatively opposite to that on the velocity profiles.

Figure 6 shows the effectiveness of R on the temperature profile. The increment in the values of R lowers the temperature profiles. Similarly, the influence of Pr on the temperature profile is shown, for the fixed values of α , β , R , and λ , in Figure 7. The sketched graph indicates a clear-cut decline in the heat profiles with increasing values of Pr .

In Figures 8-10, the impact of SL (the slip parameter) on the normal velocity, stream wise velocity and temperature profiles has been shown. It is easy to note from the graphs that both velocity profiles exhibit an increasing trend for larger values of SL , where as an opposite tendency has been seen for the temperature profiles.

Finally, Figures 11-13 display the impact of α on the velocity and temperature distributions. It is see that fluid velocity raises with increment in the values of the stretching parameter while temperature reduces as α increases.

In Figure 14, the temperature profile indicates a decrement with evolving β . Figures 15-16 are graphed to observe the effectiveness of R on the momentum curves. Both the velocity components tend to decrease by increasing the value of R .

All the values of the parameters are taken for air at room temperature, then the parameter values are varied to draw the graph (e.g., Casson fluid parameter, the thermal radiation parameter, the mixed convection parameter, the slip parameter, the shrinking/stretching parameter, and the Prandtl number).

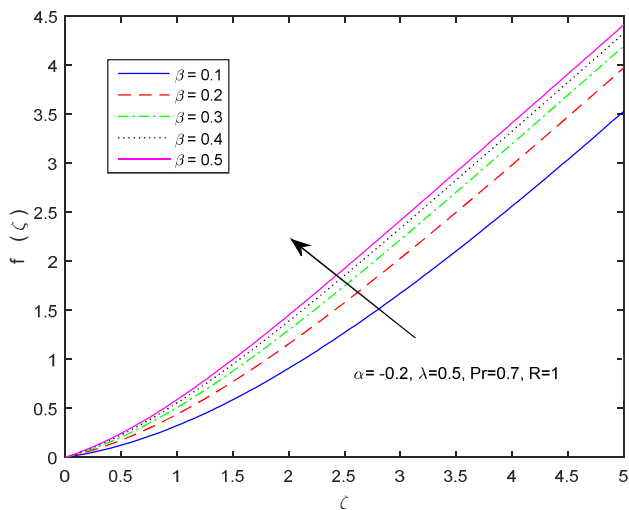


Figure 1: Normal velocity profiles for various β .

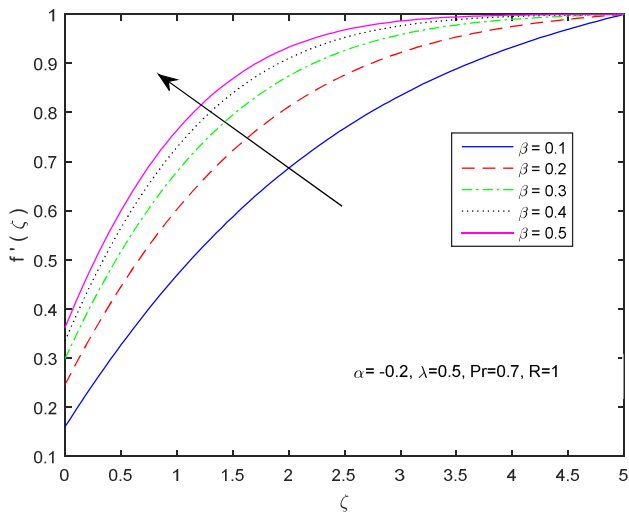


Figure 2: Streamwise velocity profiles for various β .

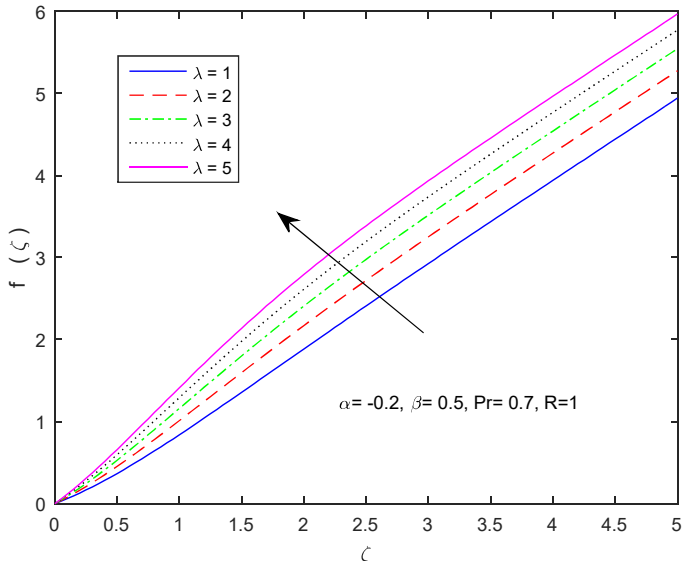


Figure 3: Normal velocity profiles for various λ .

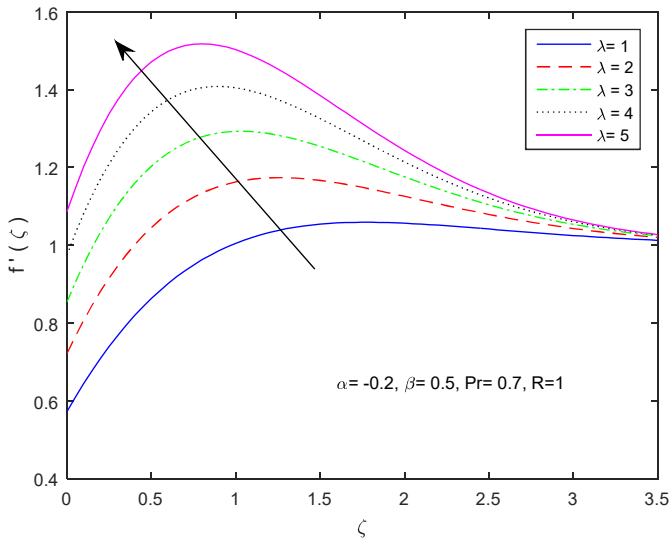


Figure 4: Streamwise velocity profiles for various λ .

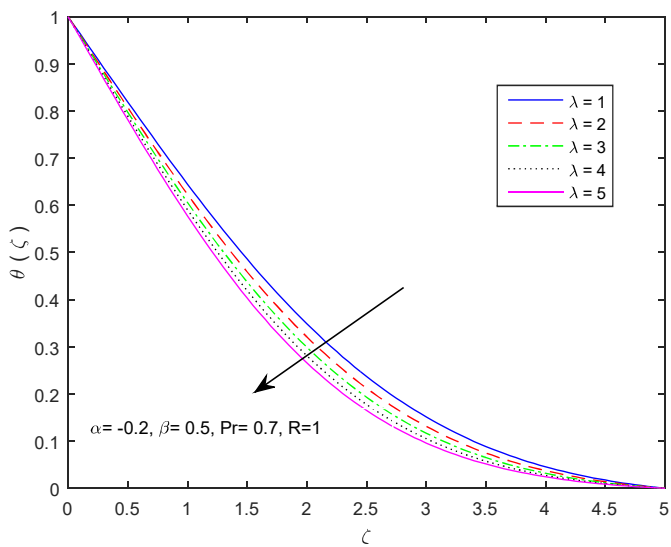


Figure 5: Temperature profiles for various λ .

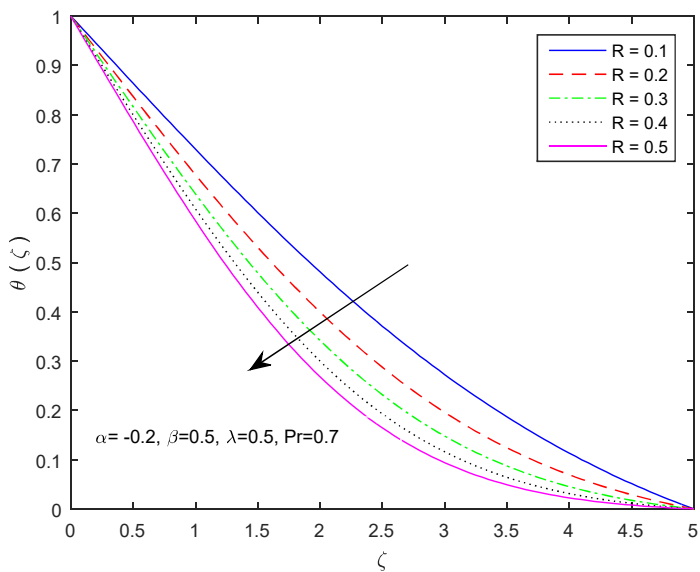


Figure 6: Temperature profiles for various R .

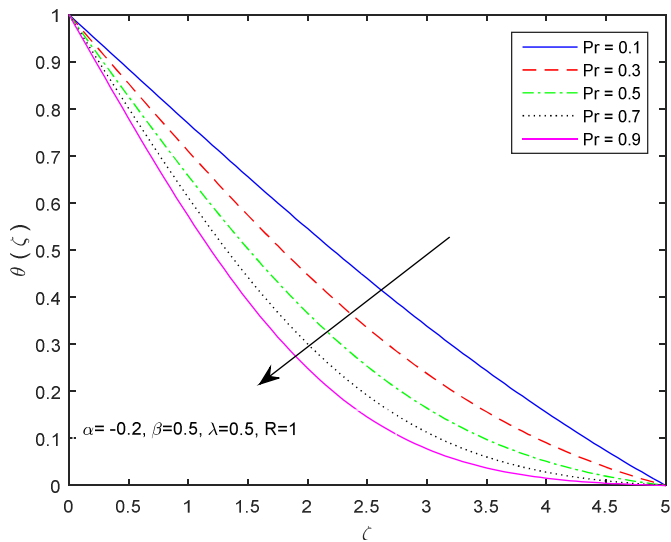


Figure 7: Temperature profiles for various Pr .

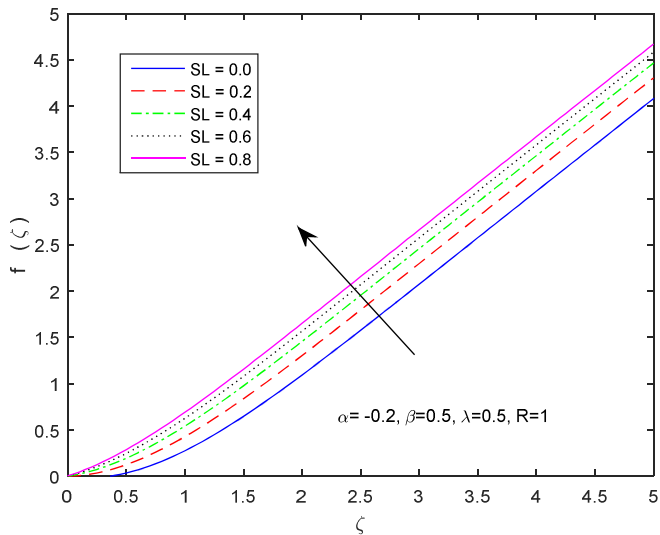


Figure 8: Normal velocity profiles for various SL .

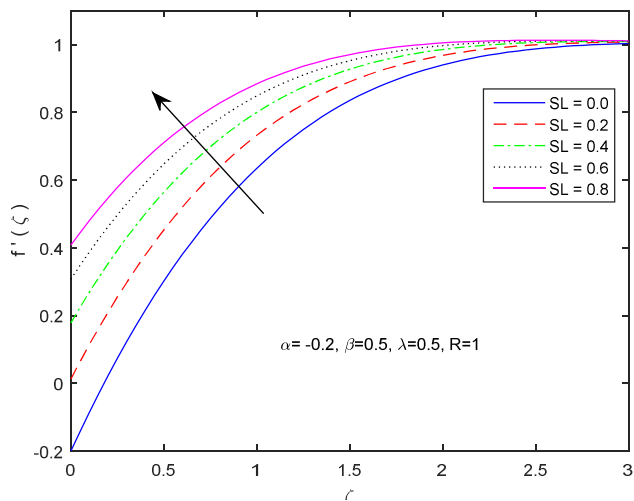


Figure 9: Streamwise velocity profiles for various SL .

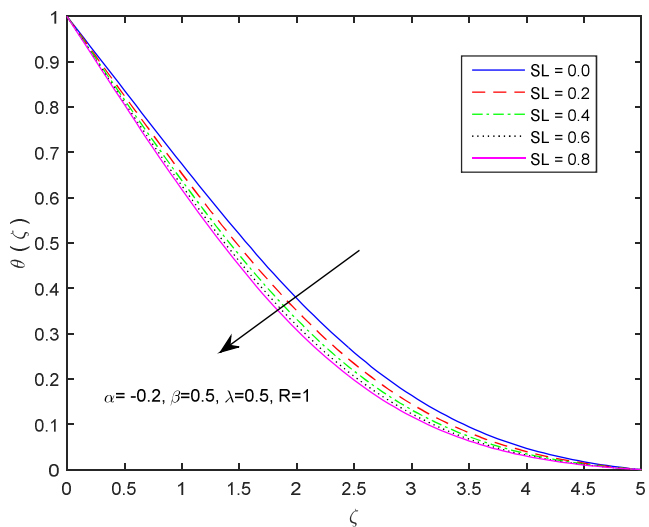
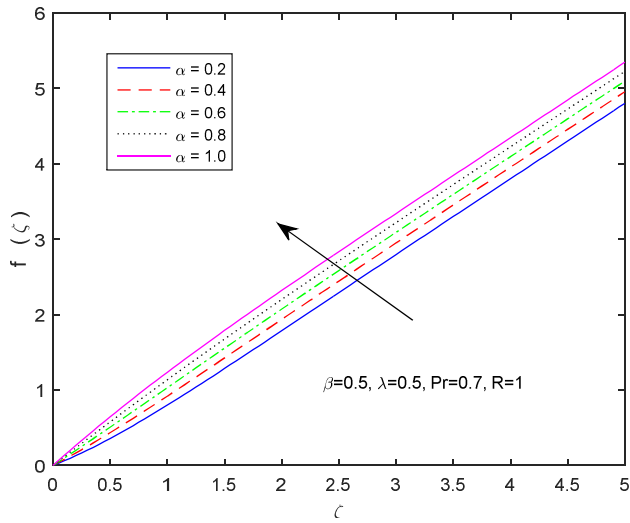
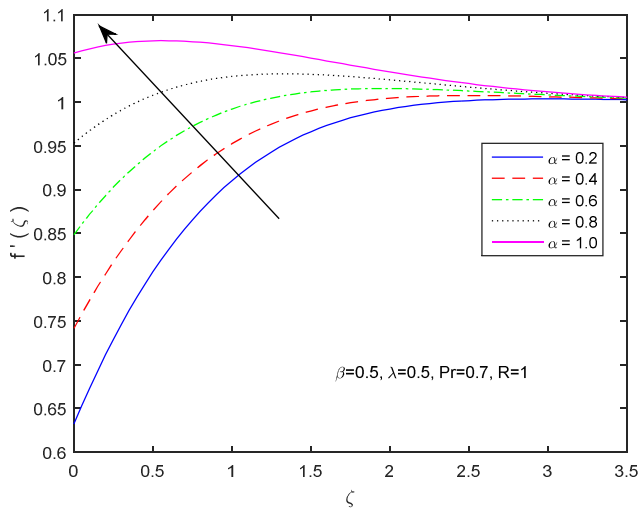


Figure 10: Temperature profiles for various SL .

Figure 11: Normal velocity profiles for various α .Figure 12: Streamwise velocity profiles for various α .

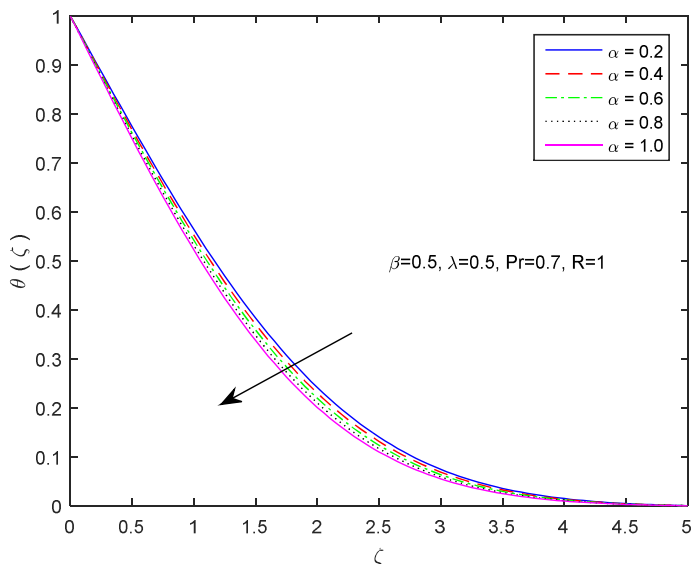


Figure 13: Temperature profiles for various α .

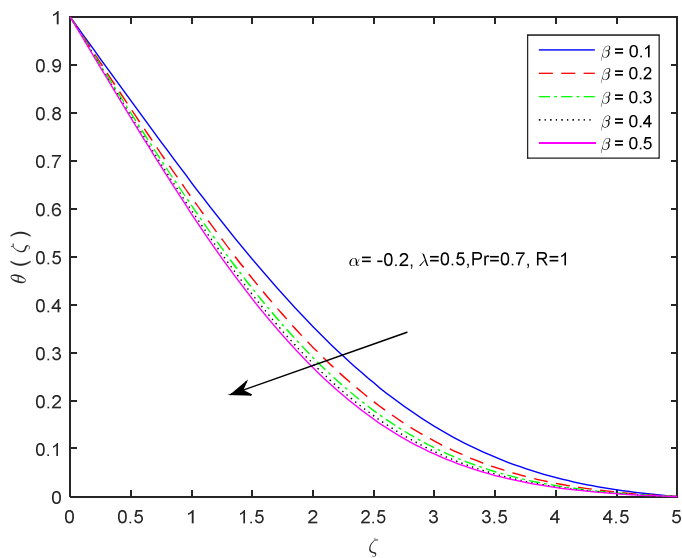
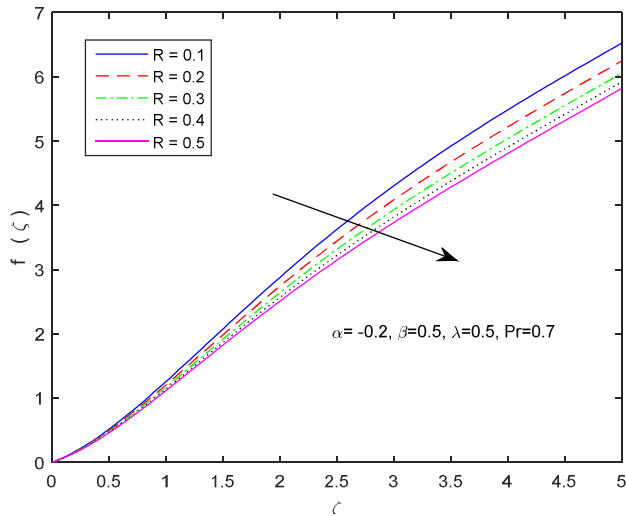
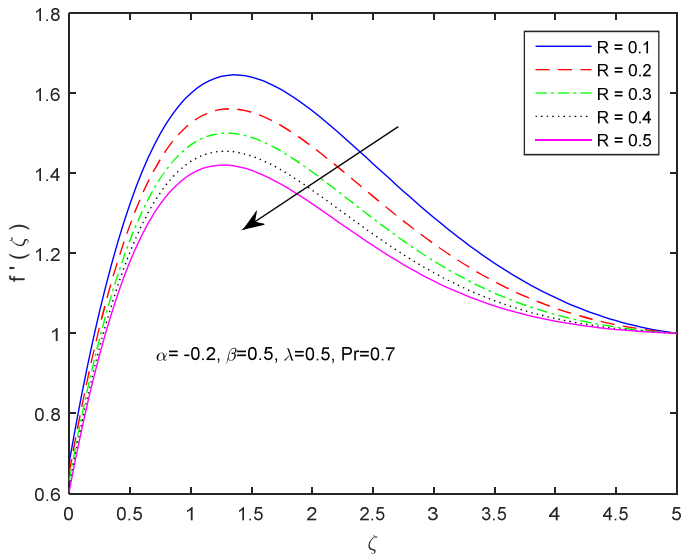


Figure 14: Temperature profiles for various β .

Figure 15: Normal velocity profiles for various R .Figure 16: Streamwise velocity profiles for various R .

Conclusions

We have numerically examined the impacts of the slip velocity and thermal radiation on the momentum and heat transfer in Casson fluid flow over a stretching surface. The

governing Navier-Stokes equations are transformed, and the solved numerically. Influence of the non-dimensional parameters has been investigated through normal velocity, stream-wise velocity and temperature profiles. Following conclusions may be drawn:

- Both the convection parameter and the Casson fluid parameter tend to accelerate the flow.
- The temperature distribution is reduced by the convection parameter, thermal radiation and the Prandtl number.
- Both velocity profiles exhibit an increasing trend for larger values of the slip parameter whereas an opposite tendency has been seen for the temperature profiles.
- Flow velocity rises with the stretching parameter while temperature reduces.

References

- [1] K. Rohlf and G. Tenti, The role of the Womersley number in pulsatile blood flow: a theoretical study of the Casson model, *Journal of Biomechanics* 34(1) (2001), 141-148. [https://doi.org/10.1016/s0021-9290\(00\)00103-2](https://doi.org/10.1016/s0021-9290(00)00103-2)
- [2] A. Mernone, V. J. N. Mazumdar and S. K. Lucas, A mathematical study of peristaltic transport of a Casson fluid, *Mathematical and Computer Modelling* 35(7-8) (2002), 895-912. [https://doi.org/10.1016/s0895-7177\(02\)00058-4](https://doi.org/10.1016/s0895-7177(02)00058-4)
- [3] Donald D. Joye, Shear rate and viscosity corrections for a Casson fluid in cylindrical (Couette) geometries, *Journal of Colloid and Interface Science* 267(1) (2003), 204-210. <https://doi.org/10.1016/j.jcis.2003.07.035>
- [4] R. R. Huilgol and Z. You, Application of the augmented Lagrangian method to steady pipe flows of Bingham, Casson and Herschel–Bulkley fluids, *Journal of Non-Newtonian Fluid Mechanics* 128(2-3) (2005), 126-143. <https://doi.org/10.1016/j.jnnfm.2005.04.004>
- [5] Adebowale Martins Obalalu, Adebayo Olusegun Ajala, Akintayo Oladimeji Akindele et al., Unsteady squeezed flow and heat transfer of dissipative casson fluid using optimal homotopy analysis method: An application of solar radiation, *Partial Differential Equations in Applied Mathematics* 4 (2021), 100146. <https://doi.org/10.1016/j.padiff.2021.100146>
- [6] J. V. Ramana Reddy, V. Sugunamma and N. Sandeep, Enhanced heat transfer in the flow of dissipative non-Newtonian Casson fluid flow over a convectively heated upper surface

- of a paraboloid of revolution, *Journal of Molecular Liquids* 229 (2017), 380-388. <https://doi.org/10.1016/j.molliq.2016.12.100>
- [7] I. Sarah Oyelakin, Sabyasachi Mondal and Precious Sibanda, Unsteady Casson nanofluid flow over a stretching sheet with thermal radiation, convective and slip boundary conditions, *Alexandria Engineering Journal* 55 (2016) 1025-1035. <https://doi.org/10.1016/j.aej.2016.03.003>
- [8] O. Daniel Makinde, Imran Ullah, Sharidan Shafie and Ilyas Khan, Unsteady MHD Falkner-Skan flow of Casson nanofluid with generative/destructive chemical reaction, *Chemical Engineering Science* 172 (2017), 694-706. <https://doi.org/10.1016/j.ces.2018.09.011>
- [9] J. Rahimi, D.D. Ganji, M. Khaki and Kh. Hosseinzadeh, Solution of the boundary layer flow of an Eyring-Powell non-Newtonian fluid over a linear stretching sheet by collocation method, *Alexandria Engineering Journal* 56 (2017), 621-627. <https://doi.org/10.1016/j.aej.2016.11.006>
- [10] A. A. Joneidi, D. D. Ganji and M. Babaelahi, Micropolar flow in a porous channel with high mass transfer, *International Communications in Heat and Mass Transfer* 36 (2009), 1082-1088. <https://doi.org/10.1016/j.icheatmasstransfer.2009.06.021>
- [11] M. Sheikholeslami and D. D. Ganji, Numerical approach for magnetic nanofluid flow in a porous cavity using CuO nanoparticles, *Materials and Design* 120 (2017), 382-393. <https://doi.org/10.1016/j.matdes.2017.02.039>
- [12] M. Sheikholeslami, Z. Ziaabakhsh and D. D. Ganji, Transport of magnetohydrodynamic nanofluid in a porous media, *Colloids and Surfaces A: Physicochemical and Engineering Aspects* 520 (2017), 201-212. <https://doi.org/10.1016/j.colsurfa.2017.01.066>
- [13] M. Sheikholeslami and D. D. Ganji, Impact of electric field on nanofluid forced convection heat transfer with considering variable properties, *Journal of Molecular Liquids* 229 (2017), 566-573. <https://doi.org/10.1016/j.molliq.2016.12.107>
- [14] M. Sheikholeslami and D. D. Ganji, Free convection of Fe₃O₄-water nanofluid under the influence of an external magnetic source, *Journal of Molecular Liquids* 229 (2017), 530-540. <https://doi.org/10.1016/j.molliq.2016.12.101>
- [15] M. Sheikholeslami and D. D. Ganji, Transportation of MHD nanofluid free convection in a porous semi annulus using numerical approach, *Chemical Physics Letters* 669 (2017), 202-210. <https://doi.org/10.1016/j.cplett.2016.12.045>
- [16] M. Fakour, A. Vahabzadeh, D. D. Ganji and M. Hatami, Analytical study of micropolar fluid flow and heat transfer in a channel with permeable walls, *Journal of Molecular Liquids* 204 (2015), 198-204. <https://doi.org/10.1016/j.molliq.2015.01.040>

- [17] S. Nadeem, Rashid Mehmood and S. S. Motsa, Numerical investigation on MHD oblique flow of Walters B type nanofluid over a convective surface, *International Journal of Thermal Sciences* 92 (2015), 162-172. <https://doi.org/10.1016/j.ijthermalsci.2015.01.034>
- [18] K. Ramesh and M. Devakar, Some analytical solutions for flows of Casson fluid with slip boundary conditions, *Ain Shams Engineering Journal* 6 (2015), 967-975. <https://doi.org/10.1016/j.asej.2015.02.007>
- [19] D. McDonald, *Blood Flows in Arteries*, 2nd edition, Arnold, London, UK, 1974.
- [20] E. Magyari and B. Keller, Heat and mass transfer in the boundary layers on an exponentially stretching continuous surface, *J. Phys. Appl. Phys.* 32 (1999), 577-585. <https://doi.org/10.1088/0022-3727/32/5/012>
- [21] S. Pramanik, Casson fluid flow and heat transfer past an exponentially porous stretching surface in presence of thermal radiation, *Ain Shams Engineering Journal* 5 (2014), 205-212. <https://doi.org/10.1016/j.asej.2013.05.003>
- [22] K. Bhattacharya, K. Vajravelu and T. Hayat, Slip effect on parametric space and the solution for the boundary layer flow of Casson fluid over a non-porous stretching/shrinking sheet, *International Journal of Fluid Mechanics Research* 40 (2013), 482-493. <https://doi.org/10.1615/interjfluidmechres.v40.i6.20>
- [23] K. Ali, S. Ahmad and M. Ashraf, Numerical simulation of flow and heat transfer in hydromagnetic micropolar fluid between two stretchable disks with viscous dissipation effects, *Journal of Theoretical and Applied Mechanics* 54 (2016), 633-643. <https://doi.org/10.15632/jtam-pl.54.2.633>
- [24] S. Ahmad, K. Ali and M. Ashraf, Heat and mass transfer analysis of MHD micropolar fluid in a channel with chemical reaction, *UPB Scientific Bulletin, Series D: Mechanical Engineering* 78(1) (2016), 131-146.
- [25] M. M. Rashidi, Muhammad Ashraf, Behnam Rostami, M. T. Rastegari and S. Bashir, Mixed convection boundary-layer flow of a micro polar fluid towards a heated shrinking sheet by homotopy analysis method, *Thermal Science* 20(1) (2016), 21-34. <https://doi.org/10.2298/tsci130212096r>

This is an open access article distributed under the terms of the Creative Commons Attribution License (<http://creativecommons.org/licenses/by/4.0/>), which permits unrestricted, use, distribution and reproduction in any medium, or format for any purpose, even commercially provided the work is properly cited.
